



Influence of Adhesive Variation and Inserts on The Strength of CFRP-to-CFRP Single Lap Bonded Joint

Kosim ABDUROHMAN^{1,*} , Rian Suari ARITONANG¹ , Rezky Agung PRATOMO² , Riki ARDIANSYAH¹ , Fajar Ari WANDONO¹ 

¹Research Center for Aeronautics Technology, National Research and Innovation Agency, 16350 Bogor, Indonesia

²Department of Metallurgy and Material Engineering, Faculty of Engineering, University of Indonesia, 16425, West Java, Indonesia

Highlights

- This paper focuses on adhesive variation and insert materials for bonded single-lap joints.
- Experimental and numerical analysis were conducted, and the results were subsequently compared.
- Adhesive with the same base material as the composite resin achieves superior bond strength.
- The chopped strand mat insert provided the best performance among the inserts.

Article Info

Received: 30 Aug 2024

Accepted: 07 Feb 2025

Keywords

Carbon Fiber
Bonded Joint
Insert
Polylactic Acid
Chopped Strand Mat

Abstract

This study aims to compare the adhesion properties of single lap joints fabricated from carbon fiber-reinforced vinyl ester composites, focusing on the effects of different adhesives and inserts. The research involved evaluating six adhesives: an aerospace-grade epoxy, two acrylic adhesives, two epoxy resins, and a vinyl ester resin. The substrates, produced via vacuum-assisted resin infusion with unidirectional carbon fiber and vinyl ester resin, were bonded using these adhesives. The impact of three inserts—3D-printed polylactic acid (PLA) nets with 0.2 mm and 0.4 mm hole spacings, and an e-glass chopped strand mat (CSM)—on the tensile properties of the SLJ was examined. Finite Element Analysis (FEA) predicted stress distributions in the joints. The results identified vinyl ester adhesive as the most suitable due to its superior lap shear strength and stiffness. Although all inserts reduced lap shear strength and modulus compared to specimens without inserts, the CSM insert showed the best performance among the inserts. The study highlights the importance of matching adhesive material to the resin used in the composite substrate, enhancing mechanical strength through better cross-linking reactions. The findings offer valuable insights for improving the design and performance of adhesively bonded joints in carbon fiber-reinforced vinyl ester composites, especially in applications requiring high strength and durability.

1. INTRODUCTION

Composites have evolved to meet standards for fatigue resistance and sustainability, offering potential for use in a wide range of applications [1]. Composites are commonly utilized in lightweight constructions, such as airplanes and automobiles, due to their specific stiffness, failure strain, and specific strength [2–7]. Composite materials have recently substituted metal and similar materials in the aerospace and aviation industries due to their excellent damping properties, low thermal expansion capacity, and superior corrosion resistance [8–10]. Their application has experienced significant growth in the automobile, maritime, wind turbine, military, civil engineering, and sports industries [2, 8, 11]. The wide range of applications for composites has sparked increased interest in developing reliable bonding methods for composite structures [2]. However, composites have limitations that restrict their application, such as high moisture absorption and low fracture toughness [12].

Joints can be classified into two main categories: adhesively bonded and mechanical joints. A bonded joint is more fatigue-resistant, does not require holes or perforations, adds less weight to the structure, and is capable of load transfer across a larger surface area than any other joint. Consequently, bonded joints are

*Corresponding author, e-mail: kosi001@brin.go.id

extensively used for joining fiber-reinforced polymer composite materials. However, bonded joints can be challenging to remove for repair and inspection, require meticulous processing of the substrate surfaces, and are influenced by operating conditions [13]. When working with adhesives, it is essential to consider diverse operational conditions, including the humidity and temperature of the area in which the bonded joints are utilized. Furthermore, during the production process, composite finishing enables the achievement of a specified geometric configuration, surface finish, precision achieved through diverse treatments, and ensures optimal bonding quality [14]. More complex and thorough surface treatment is particularly required for adhesive joining of thin or extensive areas composites [15].

Several surface treatment procedures are currently employed for composite joints, including mechanical abrasion, glass-bead abrasion technique [16], coupling agents, CO₂ laser irradiation [17], flame treatments, ultraviolet disinfection [18,19], and plasma processing [20,21]. Mechanical surface conditioning techniques, such as sanding or grit blasting, are used to improve mechanical interlocking by increasing surface roughness [22]. Hand sanding with sandpaper has been widely employed in various research studies to treat composite joint surfaces [23–31]. Furthermore, numerous studies have used grit blasting to roughen composite surfaces [32–35]. Meanwhile, other studies have evaluated a range of surface treatments, including combinations of grit and non-grit blasting [36], silicon carbide paper and plasma treatment [20], grit blasting and sanding [37], sanding and CO₂ laser irradiation [17], and peel ply-grit blasting-sanding treatment [38]. An additional investigation examined how different sandpaper grit sizes influenced the manual sanding process for composite joints [39].

The adhesively bonded joint consists of the substrate, the adhesive layer, and the interface between the substrates and the bonding agents. Enhancing the interface for specific substrates and adhesives can improve joint bond strength [40,41]. Surface properties such as substrate hardness, surface topography, and surface free energy are closely related to substrate-adhesive interfaces. These are critical parameters in adsorption, adhesion, and wettability. Furthermore, according to the theory of mechanical interlocking, when the cured adhesive penetrates and conforms to the substrate surface gaps, it creates a meshing connection with the irregular topography [42]. Surface roughness has also been found to impact mechanical interlocking, thereby enhancing bonding strength [43].

Mechanically treating surfaces with sandpaper is a simple and effective method to achieve desirable surface qualities. Dehaghani et al. found that the sanding process led to superior shear strength compared to grit blasting [37]. The study by Purnomo et al. also demonstrates the process of sanding can increase the strength of the joint of single lap joint specimens [44]. Previous studies on glass/vinyl ester composite substrates also found that the sanding process can improve the strength of single lap joints [45].

Several studies have explored the addition of insert materials to adhesive joints. Thirunavukarasu and Sikarwar conducted research on adhesively bonded single lap joints by adding unidirectional glass fiber, bidirectional glass fiber, and carbon fiber inserts [46]. Shi et al. investigated the effects of adding short Kevlar fibers to the adhesive in single lap joints [47]. Meanwhile, Pulungan et al. studied adhesively bonded composites by incorporating 3D-printed nylon inserts into double cantilever beam specimens [48]. Demircan and Kalayci investigated the effect of nano hexagonal boron nitride (h-BN) addition on the adhesion performance of epoxy adhesive in bonded joints made from GFRP and CFRP substrates [49]. It is necessary to conduct studies with insert materials different from those used in previous research to determine their influence on the performance of adhesively bonded joints of composites, as undertaken in this paper. The integration of insert materials within single lap joints in composite structures is a key area of research and development. Inserts serve multiple purposes, such as improving load transfer efficiency, preventing delamination, enhancing fatigue resistance, and enabling ease of assembly. The selection of appropriate insert materials is critical to achieving optimal joint performance under various operating conditions and environmental factors.

The purpose of this study was to compare the adhesion properties of adhesively bonded single lap joints of carbon fiber-reinforced vinyl ester composites, considering both adhesive variations and the use of inserts. The study investigated how different types of adhesives and inserts affected the tensile characteristics of single lap joints in carbon fiber/vinyl ester substrates. The specimen surfaces were sanded. Adhesive

strengths, lap shear strength with and without inserts, and fracture specimens were studied to determine the best adhesive type and insert for a carbon fiber-reinforced vinyl ester substrate. Additionally, the Finite Element Analysis was employed to forecast stress distributions in the composite joints.

The originality of this study lies in its comprehensive investigation of adhesive variation and the incorporation of inserts to optimize the performance of single lap joints (SLJs) fabricated from carbon fiber-reinforced vinyl ester composites. Unlike previous studies, this research provides a detailed comparative analysis of six adhesive types, including aerospace-grade epoxy, acrylic adhesives, epoxy-based resins, and vinyl ester resin, to evaluate their impact on the mechanical properties of SLJs. Additionally, it explores the novel use of 3D-printed polylactic acid (PLA) nets with varying hole spacings and e-glass chopped strand mat (CSM) as insert materials, offering unique insights into their influence on lap shear strength and modulus. The study integrates Finite Element Analysis (FEA) to predict stress distributions within the joints, enhancing the understanding of mechanical behavior and stress concentration zones. A significant contribution of this work is its emphasis on the critical role of adhesive-substrate compatibility. Furthermore, the research advances knowledge of mechanical interlocking and fracture behavior in bonded joints, particularly in the context of insert materials. This study highlights the importance of adhesive selection, surface preparation, and insert integration in achieving reliable and high-strength bonded composite structures.

2. MATERIAL METHOD

2.1. Materials and Substrate Manufacturing

The CFRP composite substrates were constructed using vinyl ester resin as the matrix and unidirectional carbon fiber as the reinforcement. In this investigation, vacuum-assisted resin infusion was employed, utilizing 300 gsm unidirectional carbon fiber and low-viscosity vinyl ester polymer. The vinyl ester resins were cured with the aid of Percumyl-H (cumene hydroperoxide) and P-EX (cobalt), which acted as hardeners and promoters, respectively. To manufacture the composites, various consumables were required, and a stirrer to blend vinyl ester, cobalt, and hardener until a uniform mixture was achieved.

CFRP composites with vinyl ester resin are extensively utilized in the aerospace industry. The single lap joint (SLJ) strength of these composites plays a vital role in ensuring reliable load transfer between bonded sections. One notable application of CFRP/vinyl ester composites is found in the Aerocet Amphibious Floats 1500 series, designed for Light Sport Aircraft (LSA). These floats are manufactured using the vacuum-assisted resin infusion (VARI) method, ensuring high-quality composite fabrication. Each float is produced in two parts—the top and bottom shells—which are subsequently joined through adhesive bonding. Notably, the bonded joint is strategically positioned above the at-rest waterline, ensuring structural integrity and durability in demanding operational conditions.

The Vacuum-Assisted Resin Infusion (VARI) procedure was used to create carbon fiber-reinforced polymer panels. The vinyl ester resin mixture contained 1% catalyst and 0.3% promoter by mass, and the polymer was composed of 12 layers of unidirectional carbon fabric. Composites fabricated using the VARI method achieved a fiber volume fraction of 55% and a resin volume fraction of 45%. Composite panels were cut to the dimensions outlined in ASTM D5868, employing a waterjet cutting machine to create the substrates. Each substrate measured 101.6 mm (length), 25.4 mm (width), and 3.3 mm (thickness). Ninety composite substrates were prepared, with each pair of substrates constituting a single specimen.

The specimen tabs were made from an 18-layer glass fiber/epoxy composite and were cut from composite panels measuring 25.4 mm by 25.4 mm using the same procedures as the substrates, as shown in Figure 1. Each specimen featured two tabs, one at each end. Vinyl ester resin, epoxy, glass fiber, and consumables were purchased from Justus Kimia Raya- Indonesia, while the unidirectional carbon fiber was obtained from Mitra Composites, Indonesia. The composites were manufactured at the composite facility of the Research Center for Aeronautics Technology. Material specifications for the fibers used in the substrate are as follows: 0.167 mm thickness, 100 m length, 500 mm width, 10 years shelf life, 4°C to 35°C storage conditions, 0° (unidirectional) braiding, 300 g/m² areal weight, 5800 MPa tensile strength, 255.53 GPa

tensile elastic modulus, and 1.60% elongation. Material specifications for the resins used in the substrate are as follows: 0.9 – 2.3 (Poise, 25°C) viscosity, 45 – 65 (minute, at 25°C) gel time, < 70 (°C) max. exothermic temperature, >60 (minute, at 120 °C) stability at high temperature, 100 parts resin, 0.4 part promotor P-EX, 1 part percumyl-H, M-96 rockwell hardness, 7-9 kg/mm² tensile strength, 6% tensile elongation, 110°C heat distortion temperature, 12 – 15 kg/mm² flexural strength, 270 – 300 kg/mm² flexural modulus, and 5 – 8 kg.cm/cm² charpy impact strength.



Figure 1. Specimen tabs

2.2. Adhesives and Inserts

Six types of adhesives were used in this study, including one epoxy-based aerospace-grade adhesive, two acrylic-based general adhesives, two epoxy-based resins, and a vinyl ester polymer used as the matrix for the substrate, as shown in Table 1. The type of adhesive that produces the best shear strength will be used in a follow-up study with additional inserts. The inserts to be used are two 3D-printed polylactic acid (PLA) net materials with hole spacings of 0.2 mm (see Figure 2b) and 0.4 mm (see Figure 2a), and one e-glass chopped strand mat (CSM) 450 g/m² (see Figure 2c). Material specifications for the AA (3M™ Scotch - Weld™ Epoxy Adhesive EC-2216 B/A), GA1 (Crestabond M1-30), and GA2 (Crestabond M1-20) adhesives used in this study are detailed in Table 2. The material specifications for the E1 (epoxy EPR 174) adhesives as follows: 13,000±2,000/50-100 mPa.s viscosity, 22.7±0.6 % epoxy number, 189±5 g/equiv. epoxy equivalent, 0.53±0.01 equiv./100 g epoxy value, < 0.2% total chlorine content, < 0.05% hydrolyzable chlorine content, < 1 / 2 max Colour according to the gardner scale, 1.17±0.01/1.01 g/cm³ density at 25°C, 1.572±0.003 refractive index at 25°C, < 0.2% volatile content at 3 h 140°C, < 0.1 mbar vapor pressure at 80 °C, >250 °C flashpoint, 2:1 mix ratio by weight, and curing at room temperature. The material specifications for the E2 (chempoxy resin) adhesives are as follows: 2:1 mix ratio by weight and curing at room temperature. The material specifications for the V (Ripoxy R-800 EX(VI)) adhesives are the same as the resin for the substrate. The vinyl ester resin (V) and E1 adhesives were sourced from Justus Kimia Raya Indonesia, AA was obtained from 3M, GA1 and GA2 were supplied by Scott Bader, and E2 was procured from Perdana Chemindo Indonesia.

Table 1. Adhesives

No	Adhesive types	Grade	Codes
1	Two-component epoxy	Aerospace	AA
2	Two-component acrylic	General	GA1
3	Two-component acrylic	General	GA2
4	Epoxy resin 1	General	E1
5	Epoxy resin 2	General	E2
6	Vinyl ester resin	General	V

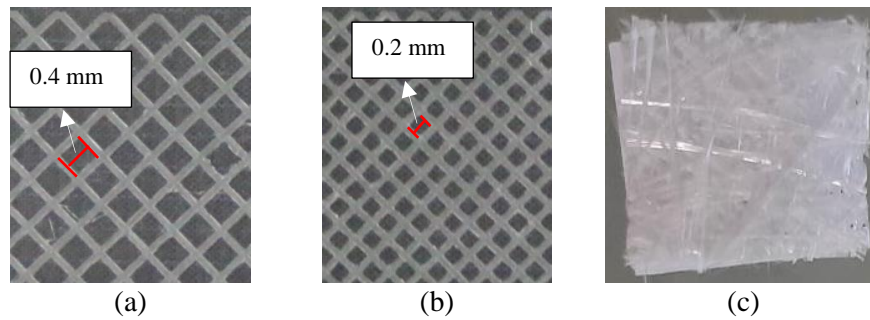


Figure 2. 3D printed PLA net 0.4 mm (a), 0.2 mm (b), and chopped strand mat (c)

Table 2. Material specification of AA, GA1, and GA2 adhesives

No	Properties	AA	GA1	GA2
1	Type	Two-component	Two-component	Two-component
2	Curing temperature	Room temperature	Room temperature	Room temperature
3	Color (visual)	White/Gray	Off-white and black	Off-white and black
4	Base	Modified epoxy/amine	Acrylic	Acrylic
5	Viscosity: (cps) (approx.)	75,000 – 150,000 / 40,000 – 80,000	100,000 - 140,000 / 80,000 – 120,000	200,000 – 240,000 / 80,000 – 120,000
6	Mix ratio by weight	5 parts / 7 parts	9:1	8.8:1
7	Mix ratio by volume	2 parts / 3 parts	10:1	10:1
8	Work life (min.)	90	25 – 35	60 – 80

2.3. Adhesive Testing

Adhesive tests were conducted on the six adhesives employed in this work to assess their tensile characteristics, with the resin-to-catalyst ratio adhering to the manufacturer's specifications. Each adhesive variation was tested using five rigid plastic specimens shaped like dog bones, under ASTM D638 standards. The samples were subjected to tensile loading at a constant speed, as shown in Figure 3. All types of adhesives will be applied to the fabrication of single lap joint (SLJ) specimens to identify the most suitable adhesives for SLJ specimens with a substrate of carbon fiber reinforced vinyl ester composite.



Figure 3. Tensile test of adhesive

2.4. Single Lap Shear Joint (SLJ) Test

The composite substrates were divided into nine groups: six for adhesive variations and three for inserts, each containing five specimens (10 substrates per group). Each substrate's surface was sanded using an 800-grit sandpaper belt (100 mm x 915 mm). Based on previous studies, a grit size of 800 has been found

to produce the best single-lap joint properties compared to other grit sizes [45]. The sanding was performed using a Rockwell belt sander set to 1700 feet per minute (fpm). After that, the treated surfaces were degreased with acetone to remove any dust and dirt. The adhesive was thoroughly combined with the hardener for two minutes before being applied to the substrate surfaces for assembly. The substrates were assembled into SLJ specimens at room temperature and categorized according to adhesive variation (see Table 3). Each SLJ specimen consisted of two substrates adhesively bonded over a 25.4 mm overlap region and held together with paper clasps. Excess adhesive within the bonded region was cleaned using a dry towel. Figure 4b illustrates the bonded area of the SLJ specimen. The specimens were maintained for 24 hours at room temperature to ensure the adhesive was fully cured. Tabs were then applied to both ends of the specimen using a similar procedure. The two tabs are inserted crossways, as illustrated in Figure 4a, to ensure direct transmission of the applied load to the specimen. The specimens were kept in a controlled dry cabinet at a humidity level of $50 \pm 5\%$ and a temperature of $23 \pm 2^\circ\text{C}$.

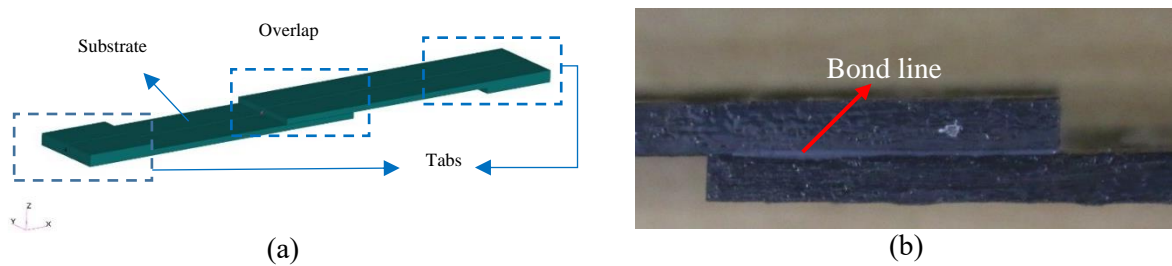


Figure 4. SLJ specimen (a) and bond line (b)

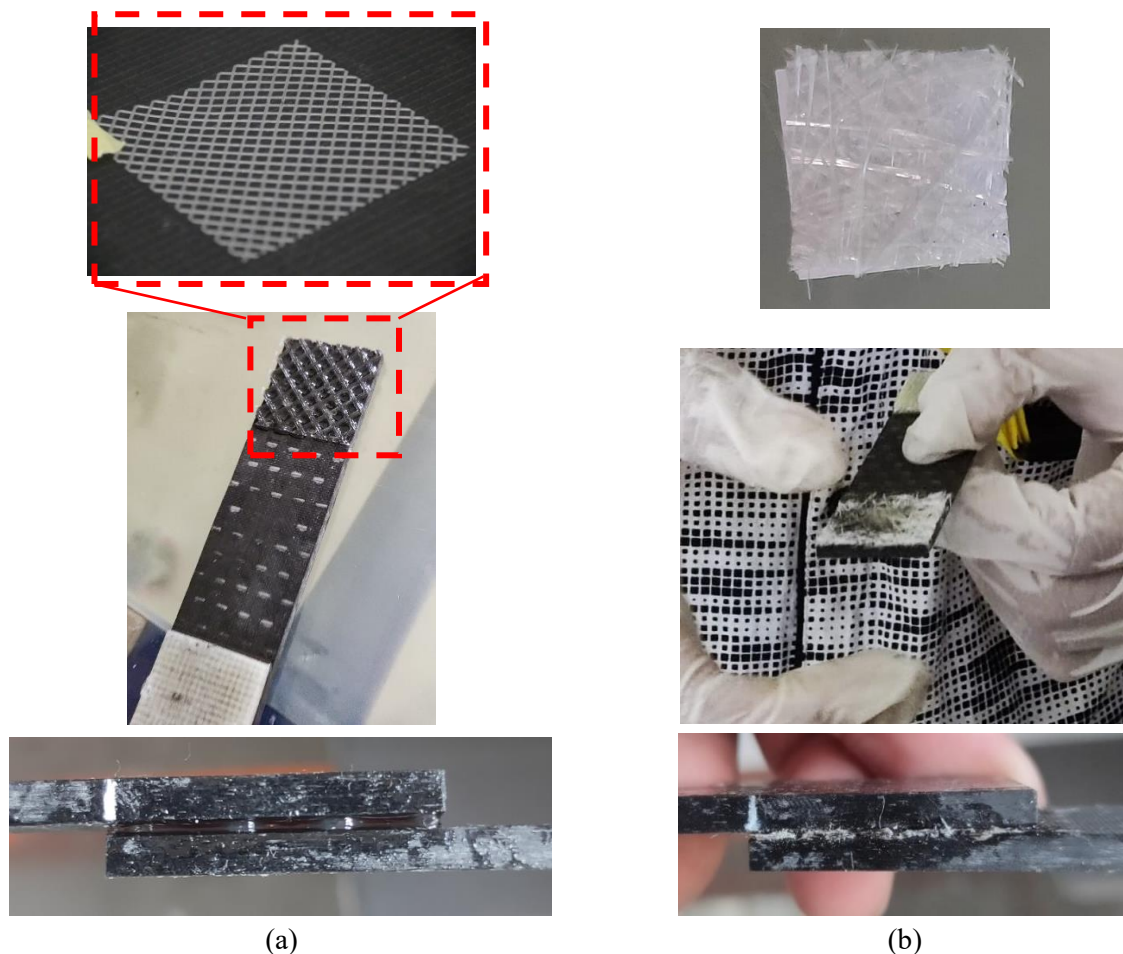


Figure 5. SLJ specimens with 3D-printed PLA net (a) and chopped strand mat (b) inserts

The lap shear strength of the CFRP-to-CFRP joints was determined using a single-lap shear adhesion test. This test was conducted on SLJ specimens with various adhesives. The tests were performed at the

Aeronautics Laboratory, PRTP-ORPA-BRIN. According to ASTM D5868, the single-lap shear test was performed utilizing a 100 kN Tensilon UTM operating at a speed of 13 mm/minute.

The most suitable adhesive for the tested carbon fiber reinforced vinyl ester substrate was selected for further study with 3D-printed PLA net inserts (0.2 mm and 0.4 mm) and chopped strand mats (CSM) inserts. The procedure for fabricating SLJ specimens with inserts is similar to that used for SLJ specimens with different adhesives. The difference is that an additional insert is included in the joint overlap area along with the selected adhesive. Figure 5a and Figure 5b illustrate the SLJ specimens with 3D-printed PLA net inserts and CSM inserts, respectively. Figures 5a and 5b illustrate that the bonding area of the SLJ specimen with the 3D-printed PLA net insert is thicker than that of the CSM insert. This difference is due to the minimum thickness limitation inherent in the manufacturing process of the net using 3D printing technology.

2.5. Finite Element (FE) Modelling

The Finite Element (FE) method is a numerical analysis approach that yields approximate solutions to various engineering problems. The primary objective of this paper is to predict the shear stress distribution within the adhesive layer of an SLJ. Using FE, the substrates were modeled as 2D plane strain shell elements, while the adhesive layer connecting the two substrates was modeled by spring elements. The FE results will be validated against experimental data.

To model the adhesive layer, two springs were placed in a grid in the middle between the substrates, acting in the x and y directions. The z-direction was not considered in this study, as the focus was solely on the shear stress distribution. The x and y directions are parallel to the overlap plane of the single lap joint. Additionally, a rigid body element was used to connect the middle grid, where the two springs are located, to the corner grid of the shell element representing the substrates. This modeling approach was originally introduced by Tahmasebi [50] to analyze bonded joints. The spring stiffness values in the x and y directions were determined based on the adhesive stress-strain curve. Since this study also includes inserts within the adhesive layer, the spring stiffness values were derived from the single lap joint stress-strain curve.

When the single lap joint model is subjected to a tensile load, it generates spring forces in the bonded joint, which can then be used to calculate the shear stress within the adhesive layer. The spring stiffness values in the x and y direction are shown in Equation (1).

$$k = \frac{AG}{t} \quad (1)$$

where in Equation (1), k is the stiffness value in the x and y direction, A is the adhesive element area, G is the shear modulus of adhesive, t is adhesive thickness. The adhesive layer shear stress can be obtained using Equation (2).

$$\tau_i = \frac{\sqrt{f_{x,i}^2 + f_{y,i}^2}}{A} \quad (2)$$

where in Equation (2), τ_i is the shear stress at element i , $f_{x,i}$ is the x direction spring force at element i , $f_{y,i}$ is the y direction spring force at element i . The shear stress values at each element along the overlap distance will be presented in a graph.

3. RESULTS AND DISCUSSION

3.1. Tensile Properties of Adhesives

Figure 6 and Table 3 present the tensile strength and modulus of various adhesives, including their standard deviations. The tensile strength values are as follows: AA at 9.11 ± 0.88 MPa, GA1 at 0.21 ± 0.03 MPa, GA2 at 0.11 ± 0.02 MPa, E1 at 54.30 ± 2.20 MPa, E2 at 47.55 ± 3.25 MPa, and V at 25.94 ± 3.8 MPa. E1

exhibits the highest tensile strength, while GA2 has the lowest. The tensile modulus values are AA at 0.3 ± 0.1 GPa, GA1 at 0.013 ± 0.009 GPa, GA2 at 0.007 ± 0.005 GPa, E1 at 2.21 ± 0.08 GPa, E2 at 2.16 ± 0.25 GPa, and V at 2.4 ± 0.22 GPa. V has the highest tensile modulus, and GA2 has the lowest. The results indicate that adhesives based on rigid plastic resins, such as E1 and V, demonstrate superior tensile properties compared to other adhesives. Despite these differences, all adhesives were applied to SLJ made of carbon fiber-reinforced vinyl ester substrates to identify the most suitable adhesive. These tensile properties are also used as material properties data for finite element analysis to predict the performance of SLJ under tensile loads.

Table 3. Tensile properties of adhesives

Adhesive Codes	Tensile Strength (MPa)	Tensile Modulus (GPa)
AA	9.11 ± 0.88	0.3 ± 0.1
GA1	0.21 ± 0.03	0.013 ± 0.009
GA2	0.11 ± 0.02	0.007 ± 0.005
E1	54.30 ± 2.20	2.21 ± 0.08
E2	47.55 ± 3.55	2.16 ± 0.25
V	25.94 ± 3.8	2.4 ± 0.22

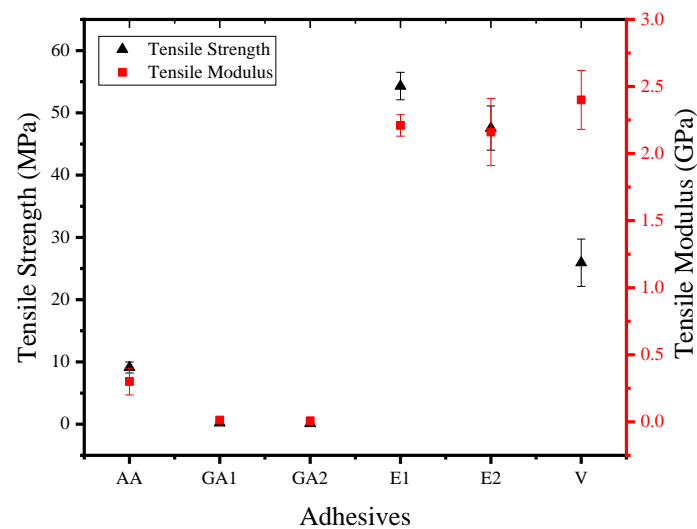


Figure 6. Tensile strength and modulus of adhesives



Figure 7. Adhesive specimens after the test

Figure 7 exhibits the fracture surface of adhesive specimens after tensile testing at a speed of 5 mm/min. The fracture appearance of rigid plastic specimens, such as those with resin-based materials, indicates a more brittle behavior compared to adhesive-based specimens. This observation is consistent with the tensile modulus values, where adhesive-based specimens (AA, GA1, and GA2) have lower tensile modulus, indicating more ductile behavior. In contrast, specimens with resin-based materials (E1, E2, and V) exhibit higher tensile moduli, suggesting a more brittle nature. The visual evidence from the fracture specimens, combined with the tensile modulus data, highlights the distinct mechanical responses between resin-based and adhesive-based materials under tensile loading.

3.2. Effect of Adhesives on SLJ Strength of CFRP

Figure 8 presents the stress vs strain relationships of single lap joint (SLJ) specimens with different adhesive variations subjected to tensile testing at a speed of 13 mm/min. SLJ specimens with AA, V, E1, and E2 adhesives exhibit a similar trend where the curve immediately drops after reaching the peak point, indicating the maximum strain point. In contrast, specimens with GA1 and GA2 adhesives show a curve that does not drop immediately after reaching the peak point but rather decreases gradually until it reaches its maximum strain. Among the adhesives, AA exhibits the highest stiffness indicated by the highest curve slope, followed by GA2, V, E1, GA1, and E2, which shows the lowest stiffness. The maximum strain observed in each specimen varies significantly, with the SLJ specimen of V displaying the highest strain at failure, indicating its ductile nature, while E1 demonstrates the lowest maximum strain, highlighting its brittle nature. In terms of lap shear strength, V reaches the highest peak stress, followed by AA, E1, GA2, E2, and GA1. These results indicate that SLJ specimens with the V adhesive provide the highest lap shear strength and strain, and comparable stiffness, while SLJ specimens with the GA1, E2, and E1 adhesives exhibit the lowest lap shear strength, stiffness, and strain, respectively.

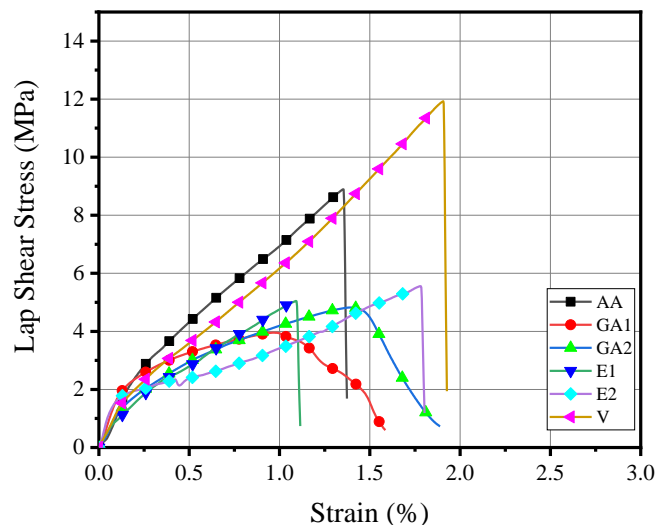


Figure 8. Stress-strain curves comparison of SLJ with adhesive variation

Figure 9 compares the shear strength and modulus of CFRP joint specimens bonded with various adhesives. The standard deviation for lap shear strength is highest for specimens with GA1 adhesive, followed by GA2, E2, E1, V, and AA. Similarly, the highest standard deviation for the modulus is observed in GA1 specimens, followed by E2, V, GA2, E1, and AA. The high standard deviation in GA1 specimens indicates significant inhomogeneity within this adhesive type, affecting the consistency and reliability of the mechanical properties. In contrast, AA specimens show the lowest standard deviation in both lap shear strength and modulus, suggesting more uniform adhesive performance. These findings highlight the variability in mechanical properties depending on the adhesive used, with GA1 exhibiting the most considerable inconsistency and AA providing the most consistent results.

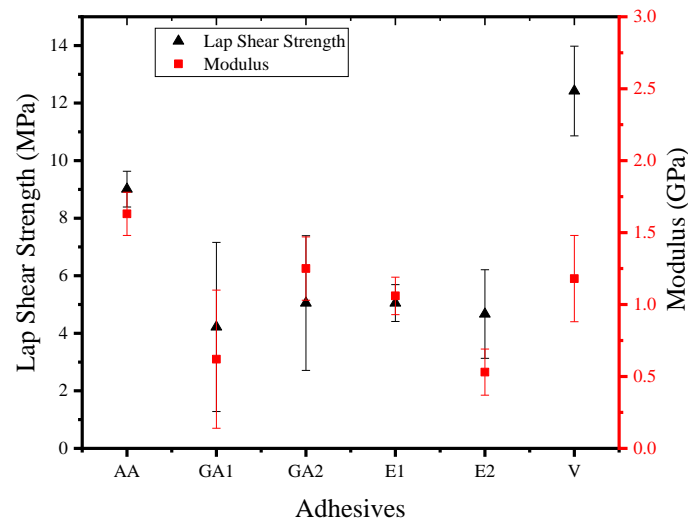


Figure 9. Shear strength and modulus comparison of SLJ with adhesive variation

Table 4 presents the lap shear strength and modulus values for SLJ specimens with various adhesives. The lap shear strength for adhesives AA, GA1, GA2, E1, E2, and V are 9.01 ± 0.62 MPa, 4.22 ± 2.94 MPa, 5.05 ± 2.34 MPa, 5.05 ± 0.64 MPa, 4.67 ± 1.54 MPa, and 12.42 ± 1.56 MPa, respectively. The modulus values for adhesives AA, GA1, GA2, E1, E2, and V are 1.63 ± 0.15 GPa, 0.62 ± 0.48 GPa, 1.25 ± 0.22 GPa, 1.06 ± 0.13 GPa, 0.53 ± 0.16 GPa, and 1.18 ± 0.3 GPa, respectively. Among these, the adhesive V exhibits the highest lap shear strength at 12.42 ± 1.56 MPa and a modulus of 1.18 ± 0.3 GPa making it the most robust choice. Adhesive AA, with a lap shear strength of 9.01 ± 0.62 MPa and a modulus of 1.63 ± 0.15 GPa, provides a balance of high shear strength and a reasonably high modulus. Therefore, adhesive V is suitable for SLJ specimens with carbon fiber-reinforced vinyl ester substrates and will be continued for further study on the effect of inserts on joint performance. However, the SLJ specimen with AA adhesive demonstrated consistent results, where the lap shear strength value of the specimen was almost equal to the tensile strength value of the adhesive itself. This indicates the consistency and reliability of aerospace-grade adhesives, although the strength value is still lower than that of SLJ specimens with V adhesives.

Table 4. Lap shear properties of SLJ with adhesive variation

Adhesive Codes	Lap Shear Strength (MPa)	Modulus (GPa)
AA	9.01 ± 0.62	1.63 ± 0.15
GA1	4.22 ± 2.94	0.62 ± 0.48
GA2	5.05 ± 2.34	1.25 ± 0.22
E1	5.05 ± 0.64	1.06 ± 0.13
E2	4.67 ± 1.54	0.53 ± 0.16
V	12.42 ± 1.56	1.18 ± 0.3

The test results indicate that the most suitable adhesive material for bonded joints is one that has the same base material as the resin used in the composite substrate. These results are consistent with previous studies, even though different base materials were used [51]. This can be attributed to the cross-linking reaction between the vinyl ester resin on the substrate and the type of adhesive used. SLJ specimens with vinyl ester adhesive exhibit a perfect cross-linking reaction between the adhesive and the resin on the substrate, resulting in a superior bond and enhanced mechanical strength. In contrast, specimens with epoxy and acrylic adhesive base materials exhibit imperfect cross-linking reactions between the vinyl ester resin on the substrate and the adhesive, leading to lower mechanical strength. This indicates that in bonded joint applications, the tensile properties of the adhesive, whether high or low, are not the only consideration, especially in single lap joints using adhesives like GA1, GA2, E1, and E2. The primary factor to consider is the similarity of the base material between the adhesive and the resin used in the composite substrate.

The results demonstrate that the choice of adhesive significantly influences the mechanical properties of SLJ joints in carbon/vinyl ester laminates, with specimens bonded using vinyl ester adhesives exhibiting superior mechanical performance compared to those bonded with other adhesives evaluated in this study. These results provide essential information for the design and application of CFRP/vinyl ester composite joints. The design process can utilize the joint property data obtained from this study to determine the appropriate joint dimensions through numerical analysis. Once the optimal joint dimensions are identified through the design process, they can then be applied to the composite structures being developed.

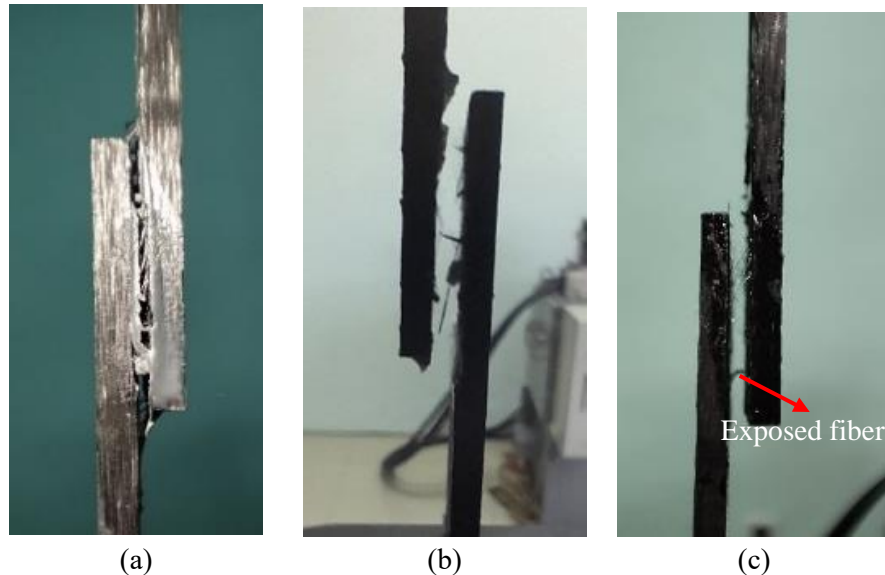


Figure 10. (a) AA, (b) E, and (c) V specimens after test

Figure 10 compares the fracture behavior of SLJ specimens with various adhesives after tensile testing. Figure 10a illustrates the fracture of specimens with adhesive AA, showing cracks in the joint area, but the substrates remain partially attached. The fracture patterns observed in specimens bonded with GA1 and GA2 adhesives are similar to those exhibited by the AA adhesive specimens. Figure 10b depicts the fracture of specimens with adhesives E1, where the substrates are completely separated. A similar fracture pattern was noted for specimens bonded with adhesive E2. Similarly, Figure 10c shows the fracture of SLJ specimens with adhesive V, with complete separation of the substrates. This indicates that SLJ joints with adhesives AA, GA1, and GA2 are more ductile, while joints with adhesives E1, E2, and V are more brittle. Notably, Figure 10c reveals exposed fibers adhering to both substrates, demonstrating that the adhesive bond with V is superior to the others, as the adhesive's strength caused the fiber layers to be exposed and remain attached to both substrates.

3.3. Effect of Inserts on SLJ Strength of CFRP

Figure 11 presents the stress vs strain relationships for SLJ specimens with adhesive V without insert and with various inserts, including 3D-printed PLA nets (0.2 mm and 0.4 mm) and chopped strand mat (CSM), after tensile testing at a speed of 13 mm/min. The specimen with vinyl ester adhesive without inserts demonstrates the highest stiffness, as evidenced by the steepest initial slope. Among the specimens with inserts, the 3D-printed PLA net of 0.2 mm shows higher stiffness compared to the 3D-printed net of 0.4 mm and the CSM. The curve indicates that the specimen with the 0.4 mm 3D-printed PLA net insert has almost a similar stiffness as the CSM insert specimen, as shown by the overlapping curves of both. The addition of inserts reduces stiffness compared to the specimen without insert, indicating that the inserts influence the load distribution within the joint.

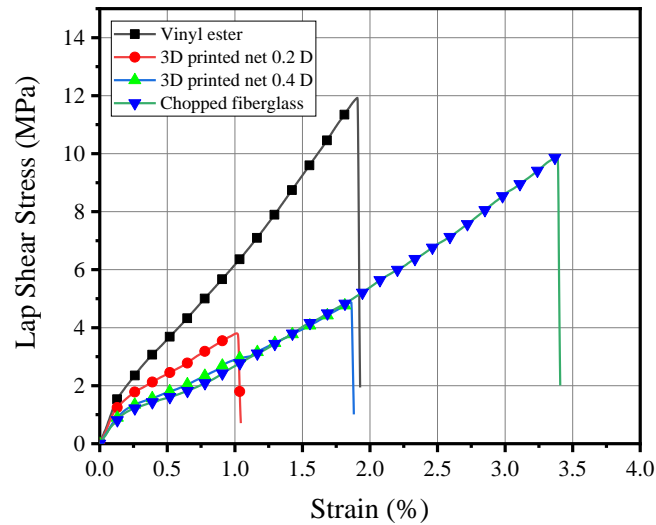


Figure 11. Stress-strain curves comparison of SLJ with inserts

Comparing the maximum strain values, the specimen with CSM exhibits the highest strain at failure, followed by the vinyl ester without insert, the 3D-printed PLA net 0.4 mm, and the 3D-printed PLA net 0.2 mm which has the lowest strain at failure. This suggests that the CSM insert contributes to higher ductility compared to the 3D-printed PLA nets. The increase in strain in specimens with glass fiber CSM inserts is consistent with studies by Thirunavukarasu and Sikarwar [46], which also observed increased strain in SLJ specimens using unidirectional and bidirectional glass fiber fabric inserts, despite the different insert materials. Another study by Shi et al. demonstrated that adding short Kevlar fibers to the adhesive also increased the strain of the SLJ specimens [47].

Regarding the peak values of lap shear strength, the specimen without insert shows the highest peak strength. Among the specimens with inserts, the CSM achieves higher lap shear strength than the 3D-printed PLA net 0.2 mm and 0.4 mm. Overall, the presence of inserts affects both stiffness and ductility, with the CSM providing a balanced improvement in strength and stiffness compared to other insert types.

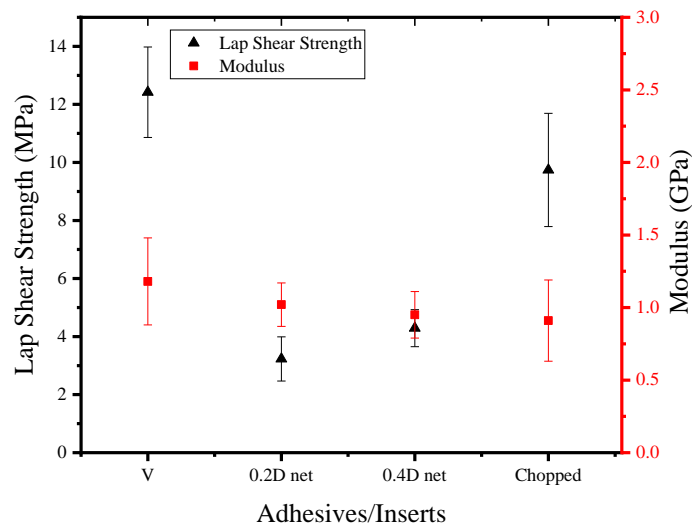


Figure 12. Shear strength and modulus comparison of SLJ with inserts

Figure 12 compares the shear strength and modulus of CFRP joint specimens using adhesive V with various inserts. The graph indicates that the highest standard deviation in lap shear strength is observed in specimens with the CSM insert, followed by specimens without insert, 3D-printed PLA net 0.2 mm insert, and finally, the the 3D-printed PLA net 0.4 mm insert. This high standard deviation in lap shear strength for the CSM specimens suggests significant variability and potential inconsistency in the mechanical properties of these

samples. Conversely, the standard deviation in modulus is highest in specimens without inserts, followed by specimens with the CSM insert, those with the 3D-printed PLA net 0.4 mm insert, and finally, those with the 3D-printed PLA net 0.2 mm insert. This indicates that specimens with the CSM insert exhibit the most considerable variation in lap shear strength, suggesting a lack of uniformity in their structural behavior. Overall, the high standard deviation values highlight the non-homogeneity of the specimens, with those containing the CSM insert showing the most significant variability in lap shear strength, and those without insert showing the most significant variability in modulus.

Table 5. Lap shear properties of SLJ with inserts

Inserts	Lap Shear Strength (MPa)	Modulus (GPa)
No insert	12.42 ± 1.56	1.18 ± 0.3
3D-printed PLA net 0.2	3.23 ± 0.76	1.02 ± 0.15
3D-printed PLA net 0.4	4.29 ± 0.64	0.95 ± 0.16
CSM	9.74 ± 1.95	0.91 ± 0.28

Table 5 presents the shear strength and modulus of CFRP joint specimens with and without various inserts. The lap shear strength values for specimens without inserts, with 3D-printed PLA net 0.2 mm inserts, 3D-printed PLA net 0.4 mm inserts, and CSM inserts are 12.42 ± 1.56 MPa, 3.23 ± 0.76 MPa, 4.29 ± 0.64 MPa, and 9.74 ± 1.95 MPa, respectively. The modulus values for these specimens are 1.18 ± 0.3 GPa, 1.02 ± 0.15 GPa, 0.95 ± 0.16 GPa, and 0.91 ± 0.28 GPa, respectively.

Comparing the lap shear strength values of specimens with inserts to those without inserts, all specimens with inserts exhibit a decrease in lap shear strength. The reductions are as follows: a 74.0% decrease for a 3D-printed PLA net of 0.2 mm, a 65.5% decrease for a 3D-printed PLA net of 0.4 mm, and a 21.6% decrease for CSM. Among the specimens with inserts, the highest lap shear strength is observed in the CSM insert specimens, while the lowest is found in the 3D-printed PLA net 0.2 mm specimens.

For modulus values, the specimens with inserts also show a decrease compared to those without inserts. The decreases are 13.6% for the 3D-printed PLA net of 0.2 mm, 19.5% for the 3D-printed PLA net of 0.4 mm, and 22.9% for CSM. Among the specimens with inserts, the highest modulus is observed in the 3D-printed PLA net 0.2 mm specimens, while the lowest is found in the CSM insert specimens.

In summary, while the addition of inserts generally reduces both lap shear strength and modulus compared to specimens without inserts, the CSM insert offers the best performance among the inserts, albeit still lower than the specimen without an insert. The 3D-printed PLA net 0.2 mm insert exhibits the lowest lap shear strength, and the CSM insert shows the lowest modulus among the inserts.

The low lap shear strength of the specimen with the 3D-printed PLA insert can be attributed to the thick bonded area, as shown in Figure 5a. This observation aligns with the study by Kahraman et al., which indicates that an increase in adhesive thickness can reduce the adhesion strength of SLJ specimens [52]. The lowest shear strength in the specimen with the 0.2 mm 3D-printed PLA insert is due to the denser PLA net, which increases the PLA volume and reduces the amount of adhesive that can bind the surfaces of the two substrates through the net holes. In contrast, the thinner CSM layer results in higher lap shear strength for specimens with this insert, demonstrating the better compatibility of e-glass fiber CSM insert material with vinyl ester adhesive compared to 3D-printed PLA material.

Figure 13 illustrates the fracture surfaces of CFRP joint specimens with various inserts after tensile testing. Figure 13a exhibits the fracture of a specimen with a 3D-printed PLA net insert, while Figure 13b shows the fracture of a specimen with a CSM insert. In Figure 13a, it can be observed that the ends of the PLA net remain adhered to one substrate, whereas the central part of the net has detached from that substrate and adhered to the other substrate. In contrast, Figure 13b shows that the CSM insert has completely detached from one substrate and adhered firmly to the other substrate. This behavior indicates that the compatibility of fiberglass material with vinyl ester adhesive is superior compare to that of PLA net, resulting in a stronger

bond between the CSM insert and the vinyl ester. This improved compatibility allows for a more robust adhesive joint with the CSM insert compared to the 3D-printed PLA net insert.

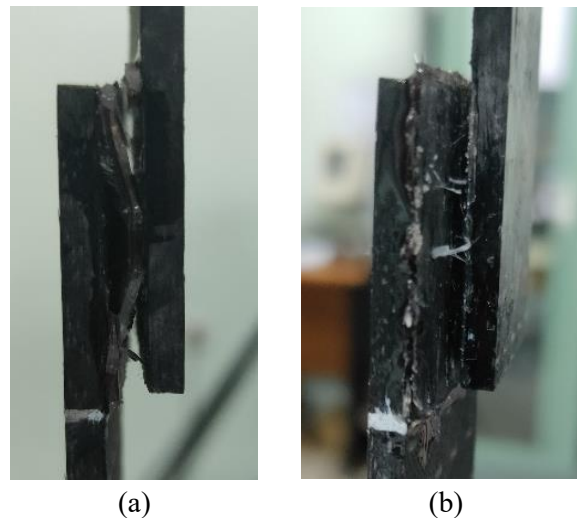


Figure 13. 3D-printed PLA net insert (a) and CSM insert (b) specimens after test

3.4. Finite Element Analysis (FEA)

The finite element analysis was employed to estimate the shear stress within the adhesive layer of the single lap joint using Patran/Nastran software. The model assumed a linear static plane strain condition. Figure 14 presents a finite element model of the SLJ, comprising spring, shell, and Rigid Body Elements (RBE). The SLJ model had 25.4 mm in width, 101.6 mm in length, and 3.3 mm in thickness. There was a total of 18 RBE, 18 spring elements, and 164 shell elements in the model. The SLJ was subjected to a tensile load at the tip of the specimen. The value of tensile load will vary depending on the type of adhesive used in the positive x-direction, as indicated by the load vs. displacement curve. The root tab was fixed and roll constraint was used in the nodes to maintain the model moves in the x-direction.

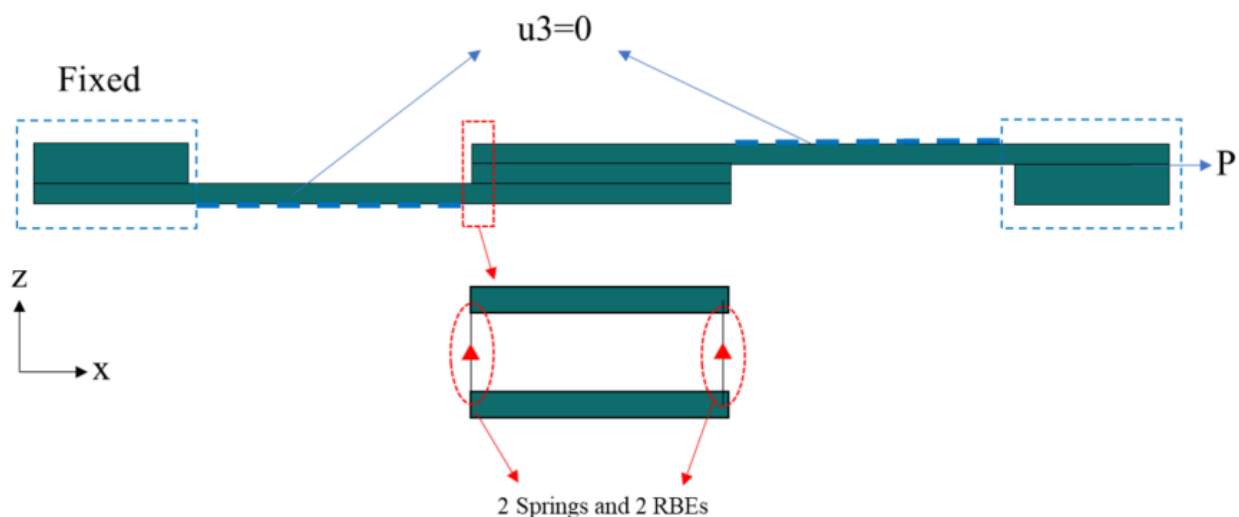
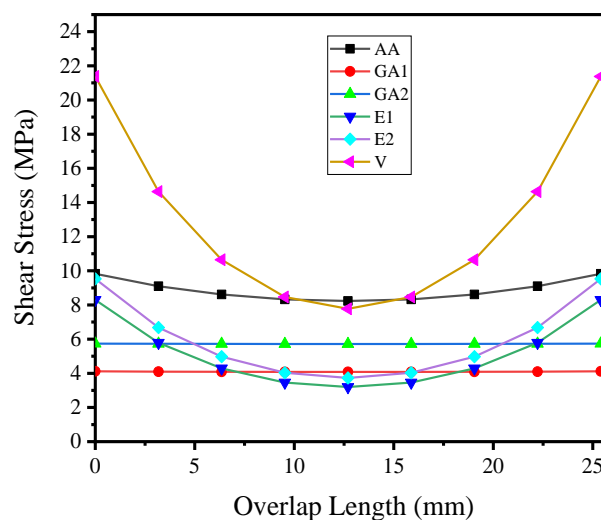


Figure 14. Finite element model of SLJ

Based on Equation (1), the parameters required for conducting an FEA simulation using linear static analysis include the overlap area, shear modulus, and adhesive thickness. The applied load varies for each type of adhesive, corresponding to the loads obtained during testing. The values for shear modulus and applied load can be found in Table 6 below. Meanwhile, the overlap area and adhesive thickness remain constant at 645.16 mm² and 0.15 mm, respectively.

Table 6. Material, geometry and load parameters for FEA

Adhesive Codes	Shear Modulus (MPa)	A (mm ²)	t (mm)	P (N)
AA	612.78	645.16	0.15	5656.6
GA1	233.08	645.16	0.15	2639.9
GA2	469.92	645.16	0.15	3692.2
E1	398.49	645.16	0.15	3109.6
E2	199.24	645.16	0.15	3598.8
V	443.61	645.16	0.15	7794.2
3D-printed PLA net 0.2	383.45	645.16	0.15	2582.9
3D-printed PLA net 0.4	357.14	645.16	0.15	3221.2
CSM	342.10	645.16	0.15	6711.2

**Figure 15.** Shear stress distribution within the adhesive layer of the SLJ specimen using various adhesive

The FE predicts the shear stress distribution within the adhesive layer of an SLJ using various adhesives as shown in Figure 15. This shear stress distribution is challenging to measure directly during SLJ testing, making the FE model a valuable tool for visualizing it. The FE analyzed six different adhesives: AA, GA1, GA2, E1, E2, and V. The results indicate that AA, GA1, and GA2 adhesives exhibit a more uniform shear stress distribution compared to E1, E2, and V adhesives, which show higher stress concentrations at the joint ends. This variation in stress distribution is attributed to the adhesives' modulus of elasticity—a lower modulus results in a more uniform shear stress distribution, while a higher modulus causes greater stress concentrations at the joint ends. However, an interesting observation is that despite the relatively high modulus of elasticity for adhesives E1 and E2, which are just below that of V (Table 3), the resulting average shear stress values for E1 and E2 are significantly lower compared to AA. This discrepancy could potentially be attributed to poor compatibility between the adhesive and the substrates. Even the strength of adhesives E1 and E2 (Table 3) drops drastically when transitioning from their original adhesive form to being applied on the SLJ specimen (Table 4).

The only type of adhesive that maintains nearly the same strength both in its original adhesive form and after being applied to the SLJ is AA. However, the AA and V adhesives still exhibit higher average shear stress values compared to the other adhesives, with values of 8.89 MPa and 13.11 MPa, respectively.

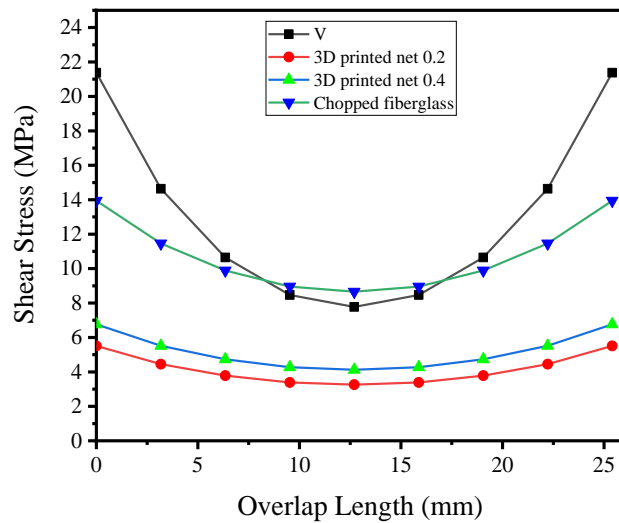


Figure 16. Shear stress distribution within the adhesive layer of the single lap joint specimen using various inserts

Figure 16 illustrates the impact of adding inserts on the shear stress distribution in the adhesive layer of the SLJ. For comparison, the shear stress distribution using the V adhesive without inserts is also included. The inserts added to the adhesive layer include a 3D printed net with 0.2 mm and 0.4 mm, as well as chopped fiberglass. The results show that the addition of these three types of inserts reduces the average shear stress when using the V adhesive. Specifically, the use of the 3D printed net with 0.2 mm and 0.4 mm decreases the average shear stress by 68.18% and 60.42%, respectively. Meanwhile, the addition of chopped fiberglass results in a 17.65% reduction in the average shear stress. This reduction is likely due to the incompatibility of these inserts with the adhesive or the substrate.

Table 7. Comparison between experimental and FEA

Adhesive Codes	Experimental Shear Strength (MPa)	FEA Shear Strength (MPa)	Error (%)
AA	9.01	8.89	1.38
GA1	4.22	4.09	2.98
GA2	5.05	5.72	13.36
E1	5.05	5.21	3.10
E2	4.67	6.02	28.85
V	12.42	13.11	5.59
3D-printed net 0.2	3.23	4.17	29.14
3D-printed PLA 0.4	4.29	5.19	20.96
Chopped Fiberglass	9.74	10.8	10.84

Table 7 presents a comparison of the average shear stress between the experimental testing and FEA results. The differences range from 1.38% to 29.14%. The smallest difference between the experimental and FEA results is observed for the AA adhesive, while the largest difference occurs with the 3D printed net 0.2 insert. These discrepancies can be attributed to several factors, including geometric and material property factors. During the fabrication of SLJ specimens, the resulting dimensions may not be identical between different specimens. In contrast, in the FE modelling, these dimensions were standardized across all specimens. Additionally, material properties might not have been consistent between the experimental results and the FE model, especially for the 3D-printed net inserts, where the properties used were those observed during SLJ testing.

The experimental results and finite element analysis provide valuable insights for designing joints when adhesives are applied in structural joint configurations. Applications requiring high shear strength should

prioritize the use of adhesives with superior mechanical properties. Conversely, for applications with lower strength requirements, adhesives with moderate strength may suffice. Additionally, ensuring compatibility between the adhesive and the composite substrate is crucial to achieving optimal joint performance and durability.

4. CONCLUSIONS

This study aimed to compare the adhesion properties of adhesively bonded single lap joints (SLJs) made from carbon fiber-reinforced vinyl ester composites, focusing on different adhesives and insert materials. The primary objectives were to investigate how various adhesives and inserts influence the tensile characteristics of these joints and to determine the most suitable adhesive and insert combination. The experimental approach included sanding the specimen surfaces, conducting tensile tests, and using Finite Element Analysis (FEA) to predict stress distributions in the composite joints.

Key findings from the study are as follows:

➤ Adhesive types and tensile properties:

- The adhesives tested included aerospace-grade epoxy, general-purpose acrylics, epoxy-based resins, and vinyl ester resin.
- Among the adhesives, the vinyl ester (V) demonstrated the highest lap shear strength and strain, indicating its suitability for SLJ applications with carbon fiber-reinforced vinyl ester substrates.
- The aerospace-grade adhesive (AA) showed consistent results and reliability, though its strength was lower than that of the vinyl ester adhesive.

➤ Influence of insert materials:

- Insert materials investigated included 3D-printed PLA nets (with 0.2 mm and 0.4 mm hole spacings) and CSM from e-glass fiber.
- The addition of inserts generally reduced both lap shear strength and modulus compared to specimens without inserts. However, the CSM insert provided the best performance among the inserts, suggesting better compatibility with the vinyl ester adhesive.

➤ Adhesive-substrate compatibility:

- The study confirmed that adhesives with the same base material as the resin in the composite substrate yield superior bond strength.
- This finding underscores the importance of material compatibility in achieving strong and reliable adhesive joints.

➤ Fracture behaviour and mechanical interlocking:

- The mechanical interlocking effect was more pronounced with adhesives and inserts that filled the substrate surface gaps effectively, resulting in stronger bonds.
- Fracture specimen analysis indicated that SLJ specimens with vinyl ester adhesive and CSM inserts exhibited better interfacial adhesion, leading to improved joint strength.

➤ Finite Element Analysis (FEA):

- FEA provided valuable insights into the stress distribution within the joints, complementing the experimental results and helping predict the performance of SLJs under tensile loads.

In conclusion, the vinyl ester adhesive emerged as the most effective for bonding carbon fiber-reinforced vinyl ester substrates, both with and without inserts. The CSM insert proved to be the most compatible and effective among the inserts tested, enhancing joint performance. This study highlights the critical role of adhesive-substrate compatibility, surface treatment, and appropriate insert selection in optimizing the adhesion properties and mechanical performance of composite joints. Future research could explore other insert materials and further refine surface treatment techniques to continue improving the strength and reliability of adhesively bonded composite joints.

ACKNOWLEDGEMENTS

The authors gratefully acknowledge the financial support for this research provided by the 'Research Organization for Aeronautics and Space,' grant No. 27/III.1/HK/2024, under the National Research and Innovation Agency- BRIN of the Republic of Indonesia.

CONFLICTS OF INTEREST

No conflict of interest was declared by the authors.

REFERENCES

- [1] Gupta, M.K., Singhal, V., Rajput, N.S., “Applications and challenges of carbon-fibres reinforced composites: a review”, *Evergreen*, 9(3): 682–693, (2015). DOI: 10.5109/4843099
- [2] Park, S.W., Lee, D.G., “Adhesion characteristics of carbon black embedded glass/epoxy composite”, *Journal Adhesion Science and Technology*, 24(4): 755–773, (2010). DOI: 10.1163/016942409X12579497420807
- [3] Yadav, N.K., Rajput, N.S., Kulshreshtha, S., Gupta, M.K., “Investigation of the mechanical and wear properties of epoxy resin composite (ERCs) made with nano particle TiO₂ and cotton fiber reinforcement”, *Evergreen*, 10(1): 63–77, (2023). DOI: 10.5109/6781041
- [4] Bindu, S., Kumar, M.P., Vinay, K.M., “Development and mechanical properties evaluation of basalt-glass hybrid composites”, *Evergreen*, 10(3): 1341–1348, (2023). DOI: 10.5109/7151681
- [5] Choudhari, D., Kakhandki, V., “Characterization and analysis of mechanical properties of short carbon fiber reinforced polyamide66 composites”, *Evergreen*, 8(4): 768–776, (2021). DOI: 10.5109/4742120
- [6] Timesli, A., “Analytical Modeling of Buckling of Carbon Nanotubes Reinforced Sandwich-Structured Composite Shells Resting on Elastic Foundations”, *Gazi University Journal of Science*, 36(4): 1700–1720, (2023). DOI: 10.35378/gujs.998265
- [7] Karacor, B., Ozcanli, M., “Examination of Fiber Reinforced Composite Materials”, *Gazi University Journal of Science*, 36(1): 301–320, (2023). DOI: 10.35378/gujs.967913
- [8] Patil, D.S., Bhoomkar, M.M., “Investigation on mechanical behaviour of fiber-reinforced advanced polymer composite materials”, *Evergreen*, 10(1): 55–62, (2023). DOI: 10.5109/6781040
- [9] Ray, S., “Effect of control parameters on erosion wear performance of glass-epoxy composites filled with waste marble powder”, *Evergreen*, 9(1): 23–31, (2022). DOI: 10.5109/4774213
- [10] Ozdemir, A. O., Subasi, M., Karatas, C., “Investigating the effects of forming parameters on molding force and springback in deep drawing process of thermoplastic composite laminates”, *Gazi University Journal of Science*, 34(2): 506–515, (2021). DOI: 10.35378/gujs.765095
- [11] Rakesh, P. K., Gupta, M. Singh, K., I., Rajput, N. S., Mahto, J. N., “fatigue strength of drilled glass fiber/epoxy laminates for bone fracture fixation”, *Gazi University Journal of Science*, 37(3): 1451–1459, (2024). DOI: 10.35378/gujs.1357147
- [12] Awi, M., Abdullah, A.S., “A review on mechanical properties and response of fibre metal laminate under impact loading (experiment)”, *Evergreen*, 10(1): 111–129, (2023). DOI: 10.5109/6781057
- [13] Kinloch, A.J., *Adhesion and Adhesives: Science and Technology*, First Edition, Cambridge University Press, (1987).
- [14] Sharma, A., Chawla, H., Srinivas, K., “Prediction of surface roughness of mild steel finished with viscoelastic magnetic abrasive medium”, *Evergreen*, 10(2): 1061–1067, (2023). DOI: 10.5109/6793663

- [15] Kim, J.K., Lee, D.G., “Adhesion characteristics of plasma-surface-treated carbon fiber-epoxy composite with respect to release films used during demolding”, *Journal Adhesion Science and Technology*, 18(4): 473–494, (2004). DOI: 10.1163/156856104323016379
- [16] Khan, M.A., Aglietti, G.S., Crocombe, A.D., Viquerat, A.D., Hamar, C.O., “Development of design allowables for the design of composite bonded double-lap joints in aerospace applications”, *International Journal of Adhesion and Adhesives*, 82(1): 221–232, (2018). DOI: 10.1016/j.ijadhadh.2018.01.011
- [17] Tao, R., Alfano, M., Lubineau, G., “In situ analysis of interfacial damage in adhesively bonded composite joints subjected to various surface pretreatments”, *Composites Part A Applied Science and Manufacturing*, 116(6): 216–223, (2019). DOI: 10.1016/j.compositesa.2018.10.033
- [18] Kupski, J., Freitas, S.T.D., Zarouchas, D., Camanho, P.P., Benedictus, R., “Composite layup effect on the failure mechanism of single lap bonded joints”, *Composite Structures*, 217(12): 14–26, (2019). DOI: 10.1016/j.compstruct.2019.02.093
- [19] Quan, D., Alderliesten, R., Dransfeld, C., Tsakoniatis, I., Freitas, S.T.D., Scarselli, G., Murphy, N., Ivankovic, A., Benedictus, R., “Significantly enhanced structural integrity of adhesively bonded PPS and PEEK composite joints by rapidly UV-irradiating the substrates”, *Composite Science and Technology*, 199(7): 108358, (2020). DOI: 10.1016/j.compscitech.2020.108358
- [20] Iqbal, S.H.M.S., Bhowmik, Benedictus, R., “Study on the effect of surface morphology on adhesion properties of polybenzimidazole adhesive bonded composite joints”, *International Journal of Adhesion and Adhesives*, 72(10): 43–50, (2017). DOI: <http://dx.doi.org/10.1016/j.ijadhadh.2016.10.002>
- [21] Katnam, K.B., Comer, A.J., Stanley, W.F., Buggy, M., Ellingboe, A.R., Young, T.M., “Characterising pre-preg and non-crimp-fabric composite single lap bonded joints”, *International Journal of Adhesion and Adhesives*, 31(7): 679–686, (2011). DOI: 10.1016/j.ijadhadh.2011.06.013
- [22] Zaldivar, R.J., Kim, H.I., Steckel, G.L., Nokes, J.P., and Patel, D.N., “The effect of abrasion surface treatment on the bonding behavior of various carbon fiber-reinforced composites”, *Journal Adhesion Science and Technology*, 26(10–11): 1573–1590, (2012). DOI: 10.1163/156856111X618425
- [23] Bautista, A., Rodriguez, J.P.C., Silva, M., Porras, A., “A dynamic response analysis of adhesive - bonded single lap joints used in military aircrafts made of glass fiber composite material under cyclic impact loading”, *International Journal of Adhesion and Adhesives*, 102(4): 102644, (2020). DOI: 10.1016/j.ijadhadh.2020.102644
- [24] Zhang, J., Cheng, X., Guo, X., Bao, J., Huang, W., “Effect of environment conditions on adhesive properties and material selection in composite bonded joints”, *International Journal of Adhesion and Adhesives*, 96(12): 1–7, (2020). DOI: 10.1016/j.ijadhadh.2018.12.001
- [25] Huang, W., Sun, L., Liu, Y., Chu, Y., Wang, J., “Effects of low-energy impact at different temperatures on residual properties of adhesively bonded single-lap joints with composites substrates”, *Composite Structures*, 267(2): 113860, (2021) DOI: 10.1016/j.compstruct.2021.113860
- [26] Choudhury, M.R., Debnath, K., “Experimental analysis of tensile and compressive failure load in single-lap adhesive joint of green composites”, *International Journal of Adhesion and Adhesives*, 99(11), (2020). DOI: 10.1016/j.ijadhadh.2020.102557

- [27] Hu, C., Huang, G., Li, C., “Experimental and numerical study of low-velocity impact and tensile after impact for cfrp laminates single-lap joints adhesively bonded structure”, *Materials (Basel)*, 14(4): 1–24, (2021). DOI: 10.3390/ma14041016
- [28] Freitas, S.T.D., Sinke, J., “Failure analysis of adhesively-bonded skin-to-stiffener joints : metal – metal vs composite – metal”, *Engineering Failure Analysis*, 56: 2–13, (2015). DOI: <http://dx.doi.org/10.1016/j.engfailanal.2015.05.023>
- [29] Akpınar, I.A., Gültekin, K., Akpınar, S., Akbulut, H., Ozel, A., “Research on strength of nanocomposite adhesively bonded composite joints”, *Composites Part B Engineering*, 126: 143–152, (2017). DOI: 10.1016/j.compositesb.2017.06.016
- [30] Sun, C., Jia, P., Chen, C., Moradi, A., Zhou, J., Al Teneiji, M., Cantwell, W.J., Guan, Z.W., “The effect of carbon fibre stitching on the tensile behaviour of secondary bonded single- and double-lap composite joints”, *Composite Structures*, 26(12): 113774, (2021). DOI: 10.1016/j.compstruct.2021.113774
- [31] Sugiman, S., Setyawan, P.D., Salman, S., Ahmad, H. “Experimental and numerical investigation of the residual strength of steel-composites bonded joints: effect of media and aging condition”, *Composites Part B Engineering*, 173(5), (2019). DOI: 10.1016/j.compositesb.2019.106977
- [32] Fawcett, A., Chen, X., Huang, X., Li, C., “Failure analysis of adhesively bonded GFRP/ aluminum matrix single composite lap joint with cold worked penetrative reinforcements”, *Composites Part B Engineering*, 161(7): 96–106, (2019). DOI: 10.1016/j.compositesb.2018.10.051
- [33] Ramaswamy, K., O’Higgins, R. M., McCarthy, M.A., McCarthy, C. T., “Influence of adhesive spew geometry and load eccentricity angle on metal-composite bonded joints tested at quasi-static and dynamic loading rates”, *Composite Structures*, 279(2): 114812, (2022). DOI: 10.1016/j.compstruct.2021.114812
- [34] Freitas, S.T.D., Banea, M.D., Budhe, S., Barros, S.D., “Interface adhesion assessment of composite-to-metal bonded joints under salt spray conditions using peel tests”, *Composite Structures*, 164: 68–75, (2017). DOI: 10.1016/j.compstruct.2016.12.058
- [35] Grefe, H., Kandula, M.W., Dilger, K., “Influence of the fibre orientation on the lap shear strength and fracture behaviour of adhesively bonded composite metal joints at high strain rates”, *International Journal of Adhesion and Adhesives*, 97, (2020). DOI: 10.1016/j.ijadhadh.2019.102486
- [36] Ramaswamy, K., O’Higgins, R.M., Kadiyala, A.K., McCarthy, M.A., McCarthy, C.T., “Evaluation of grit-blasting as a pre-treatment for carbon-fibre thermoplastic composite to aluminium bonded joints tested at static and dynamic loading rates”, *Composites Part B Engineering*, 185(1): 107765, (2020 DOI: 10.1016/j.compositesb.2020.107765
- [37] Dehaghani, R.C., Cronin, D., Montesano, J., “Performance and failure assessment of adhesively bonded non-crimp fabric carbon fiber/epoxy composite single lap joints”, *International Journal of Adhesion and Adhesives*, 105: 102776, (2021). DOI: 10.1016/j.ijadhadh.2020.102776
- [38] Sorrentino, L., Polini, W., Bellini, C., Parodo, G., “Surface treatment of CFRP: influence on single lap joint performances”, *International Journal of Adhesion and Adhesives*, 85(5): 225–233, (2018). DOI: 10.1016/j.ijadhadh.2018.06.008
- [39] Yang, G., Yang, T., Yuan, W., Du, Y., “The influence of surface treatment on the tensile properties of carbon fiber-reinforced epoxy composites-bonded joints”, *Composites Part B Engineering*, 160(7): 446–456, (2019). DOI: 10.1016/j.compositesb.2018.12.095

- [40] Gude, M.R., Prolongo, S.G., Ureña, A., “Adhesive bonding of carbon fibre/epoxy laminates: Correlation between surface and mechanical properties”, *Surface and Coatings Technology*, 207(3): 602–607, (2012). DOI: 10.1016/j.surfcoat.2012.07.085
- [41] Rhee, K.Y., Lee, S.G., Choi, N.S., Park, S.J., “Treatment of CFRP by IAR method and its effect on the fracture behavior of adhesive bonded CFRP/aluminum composites”, *Materials Science and Engineering: A*, 357(1–2): 270–276, (2003). DOI: 10.1016/S0921-5093(03)00207-7
- [42] Baldan, A., “Adhesion phenomena in bonded joints”, *International Journal of Adhesion and Adhesives*, 38: 95–116, (2012). DOI: 10.1016/j.ijadhadh.2012.04.007
- [43] Zhan, X., Li, Y., Gao, C., Wang, H., Yang, Y., “Effect of infrared laser surface treatment on the microstructure and properties of adhesively CFRP bonded joints”, *Optics & Laser Technology*, 106: 398–409, (2018). DOI: 10.1016/j.optlastec.2018.04.023
- [44] Purnomo, H., Rifa'i, M.J., Purwoko, Vicarneltor, D.N., Ibadi, M., Setianto, M.H., Yudanto, M., Rizkyta, A.G., “Implementing surface treatment and adhesive variations for bonded joints between composite GFRP and aluminum at 200 °C”, *Eastern-European Journal of Enterprise Technologies*, 1(127): 60–66, (2024). DOI: 10.15587/1729-4061.2024.297904
- [45] Abdurohman, K., Pratomo, R.A., Hidayat, R., Ramadhan, R.A., Nurtiasto, T.S., Ardiansyah, R., Pratama, M.G.P.P., Wandono, F.A., “Influence of abrasion treatments on performance of adhesively bonded glass/vinyl ester single lap joints”, *Evergreen*, 11(2): 806–820, (2024). DOI: 10.5109/7183361
- [46] Thirunavukarasu, A., Sikarwar, R.S., “Enhancing the strength of adhesively bonded single-lap composite joints using fiber fabrics”, *Materials Letters*, 357(9), (2024). DOI: 10.1016/j.matlet.2023.135664
- [47] Shi, S., Liu, Z., Lv, H., Zhou, X., Sun, Z., Chen, B., “The tensile properties of adhesively bonded single lap joints with short kevlar fiber”, *International Journal of Adhesion and Adhesives*, 134: 1–9, (2024). DOI: <https://doi.org/10.1016/j.ijadhadh.2024.103794>
- [48] Pulungan, D., Andika, S., Dirgantara, T., Wirawan, R., Judawisastra, H., Wicaksono, S., “Promoting bridging in adhesively bonded composites with polymer inserts: A computational perspective”, *Composites Part A: Applied Science and Manufacturing*, 180(11), (2024). DOI: 10.1016/j.compositesa.2024.108107
- [49] Demircan, O., Kalaycı, A., “Investigation of mechanical properties of nano hexagonal boron nitride integrated epoxy adhesives in bonded GFRP and CFRP composite joints”, *International Journal of Adhesion and Adhesives*, 133, (2024). DOI: 10.1016/j.ijadhadh.2024.103759
- [50] Tahmasebi, F., “Automation tools for finite element bonded joints analysis of adhesively bonded joint”, *JSME/ASME International Conference on Materials and Processing*, 322–326, (2002).
- [51] Gunawan, A., Widanto, M., Abdurohman, K., Pratomo, R.A., “Effect of adhesive types and fiber orientation on mechanical properties of single lap joint composite using vacuum-assisted resin infusion manufacturing method”, *Aviner* (2024). DOI: 10.4108/eai.8-11-2023.2345855
- [52] Kahraman, R., Sunar, M., Yibas, B., “Influence of adhesive thickness and filler content on the mechanical performance of aluminum single-lap joints bonded with aluminum powder filled epoxy adhesive”, *Journal of Materials Processing Technology*, 205(1–3): 183–189, (2008). DOI: 10.1016/j.jmatprotec.2007.11.121